

Earthquake Hazard After a Mainshock in California

PAUL A. REASENBERG AND LUCILE M. JONES

After a strong earthquake, the possibility of the occurrence of either significant aftershocks or an even stronger mainshock is a continuing hazard that threatens the resumption of critical services and reoccupation of essential but partially damaged structures. A stochastic parametric model allows determination of probabilities for aftershocks and larger mainshocks during intervals following the mainshock. The probabilities depend strongly on the model parameters, which are estimated with Bayesian statistics from both the ongoing aftershock sequence and from a suite of historic California aftershock sequences. Probabilities for damaging aftershocks and greater mainshocks are typically well-constrained after the first day of the sequence, with accuracy increasing with time.

IN THE IMMEDIATE AFTERMATH OF A large earthquake in a populated region, numerous decisions will have to be made concerning the suspension and resumption of critical services, including the operation of utilities, industrial processes, transportation facilities, and schools. The need to resume these activities and to reoccupy structures that may have been weakened or partially damaged in the mainshock must be tempered by the expectation that one or more additional damaging earthquakes, including either a second, larger mainshock or one or more strong aftershocks, may occur (1, 2). Although most of the structural damage associated with an earthquake sequence occurs during the mainshock shaking, significant additional damage and loss of life has been sustained during strong aftershocks, particularly in structures weakened by the mainshock. Reliably assessing the extent of structural damage sustained in the mainshock for a particular structure may take several weeks or more. However, the need to reoccupy that structure may be urgent. To approach rationally the questions of when to resume certain activities and which structures to reoccupy, we must be able to assess the probabilities for the occurrence of both a larger mainshock and strong aftershocks.

The probability that a larger earthquake will follow an earthquake of a given magnitude has been estimated empirically for the southern California region from the occurrence rate of foreshocks (3). State and federal hazard evaluation and emergency response officials have included this assess-

ment of the enhanced probability of a larger earthquake in responding to recent moderate events in California (4). We have developed a parametric model in which we describe stochastically an earthquake sequence and derive a probability for the occurrence of either a larger mainshock or a strong aftershock. Our model is based on data from California earthquakes, but can be applied elsewhere.

The distributions of aftershocks in space, time, and magnitude follow well-known stochastic laws (2, 5-9). Indeed, aftershocks can be identified only in a statistical fashion; they bear no known characteristics differentiating themselves from other earthquakes. In general, the rate of occurrence of earthquakes increases abruptly after a mainshock, and then decreases with time after the mainshock according to a power-law decay, while the earthquake magnitudes have an expo-

ponential distribution that is stationary in time (Fig. 1). We use these relations to model earthquake sequences and to estimate probabilities for the occurrence of strong aftershocks or larger mainshocks in any given time interval. We consider the combined probability that one or more additional earthquakes (strong aftershock or larger mainshock) will occur in a given magnitude range and time interval. We do not distinguish between the case of one such event occurring and that of more than one occurring; we assume that virtually all questions of public policy would have the same outcome in either case.

We model the aftershock process as a nonhomogeneous Poisson process in time with intensity, $N(t)$, obeying the modified Omori law (7)

$$N(t) = \frac{K}{(t+c)^p} \quad (1)$$

where t is time after the mainshock, and K , c , and p are constants. We model the magnitude distribution following the Gutenberg-Richter relation

$$N(M) = A \cdot 10^{-bM} \quad (2)$$

where M is the aftershock magnitude, and A and b are constants. Then the rate, λ , of aftershocks with magnitude M or larger, at the time t following a mainshock of magnitude M_m , may be expressed as

$$\lambda(t, M) = 10^{a+b(M_m-M)}(t+c)^{-p} \quad (3)$$

where a , b , p , and c are constants. The probability, P , of one or more earthquakes occurring in the magnitude range ($M_1 \leq M < M_2$) and time range ($S \leq t < T$) is

$$P = 1 - \exp \left[- \int_{M_1}^{M_2} \int_S^T \lambda(t, M) dt dM \right] \quad (4)$$

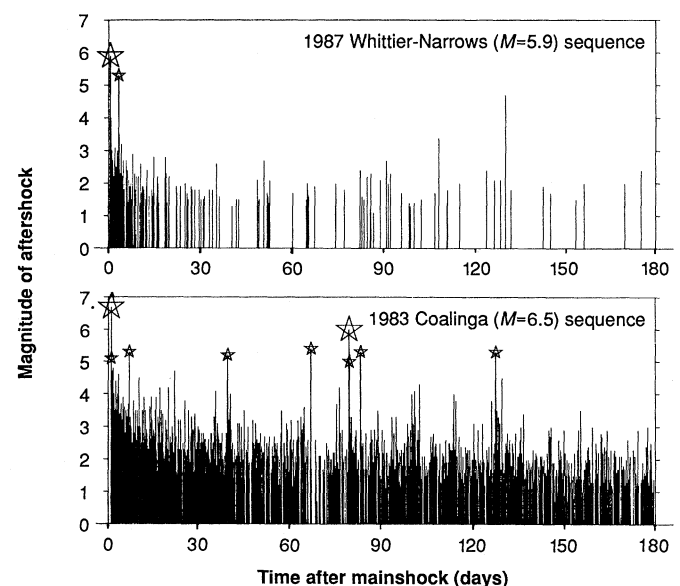


Fig. 1. Aftershock activity following two recent California earthquakes. (A) 1 October 1987 ($M = 5.9$) Whittier-Narrows earthquake. (B) 2 May 1983 ($M = 6.5$) Coalinga earthquake. Small stars indicate $M \geq 5.0$ events; large stars, $M \geq 5.5$ events.

P. A. Reasenber, U.S. Geological Survey, 345 Middlefield Road, Mail stop 977, Menlo Park, CA 94025.
L. M. Jones, U.S. Geological Survey, 525 South Wilson Avenue, Pasadena, CA 91106.

We estimate the interval probabilities $P(M_1, M_2, S, T)$ by evaluating Eq. 4 over selected time and magnitude intervals, using point estimates of the constant model parameters. Probabilities for aftershocks are obtained when $M_2 = M_m$. Probabilities for a larger mainshock are obtained when $M_1 = M_m$ and $M_2 = \infty$ (Tables 1 and 2).

We have estimated the parameters in Eq. 3 using earthquake data from California (11–14). We identified 62 aftershock sequences ($M_m \geq 5$) occurring from 1933 to 1987 using a cluster recognition algorithm (10, 15). Model parameters were estimated separately for each sequence with the method of maximum likelihood. We used all aftershocks with $M \geq M_m - 3$ to determine the fit to Omori's Law (parameters a and p); we used all aftershocks with $M \geq 2$ to determine parameter b (16). Mean parameter values determined for these 62 sequences are $\bar{b} = 0.90 \pm 0.02$, $\bar{p} = 1.07 \pm 0.03$, and $\bar{a} = -1.76 \pm 0.07$ (17) (Fig. 2). These values are similar to those obtained from comparable aftershock sequences worldwide. Ranges and median value of b are 0.51 to 1.33, median 0.83 for 13 sequences in Japan; 0.46 to 1.00, median 0.82 for 10 sequences in Southern California; and 0.56 to 1.36, median 0.82 for 10 sequences in Greece (7). The range of most commonly reported values of p worldwide is ~ 1.0 to ~ 1.4 . Earthquake sequences in eastern California had significantly higher values of a than their counterparts in both the compressional regime of southern California and the strike-slip regime of central California, which implies that there is a higher probability for aftershocks in eastern California sequences (18). We refer to the distributions of parameter values determined for the 62 historic California sequences as the a priori distributions. The set of model parameters consisting of the medians of the a priori distributions ($a = -1.67$, $b = 0.91$, $p = 1.08$, $c = 0.05$) is termed the "generic California" model (Fig. 2; Table 1).

Estimated interval probabilities for the generic sequence indicate that most large aftershocks (those with magnitude one unit below the mainshock or greater) occur within a few weeks of the mainshock, and are approximately seven times as likely as a greater mainshock in any given interval (Table 1). For example, the estimated probability that at least one $M \geq 5.5$ earthquake will follow a $M = 6.5$ mainshock in a generic sequence during the 1-week interval beginning 0.01 day after the mainshock is 0.34. After 15 days, the 1-week probability drops to 0.03. The estimated probability for the occurrence of a larger mainshock in the 30-day interval beginning 0.25 days after the mainshock is 0.04 (19).

Primary support for the validity of the generic model for earthquakes with magnitude larger than the mainshock is obtained independently from the empirical frequency of foreshocks. During the first 7-day interval following $M \geq 5.0$ earthquakes in southern California, the probability (determined from the foreshock occurrence rate) that another earthquake of equal or greater magnitude will occur is 0.056 (20). The corresponding probability estimated with the generic California model is 0.049 (Table 1). The agreement between these estimates for the immediate probability of a larger mainshock provides some confidence that our model is approximately valid in this extended magnitude range. Thus, the generic model provides a useful starting point for estimating post-mainshock hazard in the absence of any information about a particular sequence other than the mainshock magnitude. However, departures from this generic behavior are expected in any given aftershock sequence.

Two recent earthquake sequences serve to illustrate such departures: the 1983 ($M = 6.5$) Coalinga earthquake and the 1987 ($M = 5.9$) Whittier-Narrows earthquake (21–23). The magnitude distributions for these sequences differed slightly ($b = 0.73$ for Whittier-Narrows, $b = 0.89$ for Coalinga). The Coalinga sequence was more productive in aftershocks ($a = -1.47$) than the Whittier-Narrows sequence ($a = -1.60$), and the decay in its rate of aftershocks was slower ($p = 1.06$ for Coalinga; $p = 1.50$ for Whittier-Narrows). These contrasts in model parameters account for substantial differences in the resulting probability estimates, both between these sequences and relative to the generic sequence, and illustrate the variation of hazard among California earthquake sequences (Table 2) (24). For example, the calculated probability for the occurrence of one or more $M \geq 4.9$ events at Whittier-Narrows during the 1-week beginning 1 day after the mainshock was 0.10 (Table 2); one aftershock in this magnitude range occurred 2.8 days after the Whittier-Narrows mainshock (Fig. 1A). At Coalinga, the estimated probability for one or more $M \geq 5.5$ events during the 90-days beginning 1 day after the mainshock was 0.39; one strong aftershock ($M = 5.8$) occurred at Coalinga 80 days after the mainshock (Fig. 1B).

A much more practical use of the model is the calculation of interval probabilities for aftershocks or larger mainshocks in real time during an ongoing aftershock sequence. The model parameters for an ongoing earthquake sequence can be estimated with Bayes rule (25, 26). We assume that the a priori estimates of each parameter, θ , are normally

distributed with some mean value θ_0 and variance σ_0^2 , and that the a posteriori estimate of the parameter, determined from a sample of size n , is normally distributed with some mean $\hat{\theta}$ and variance σ^2 . Then the Bayesian estimate of θ , for a mean squared error loss function, is given by

$$\hat{\theta}_B = \left(\frac{\sigma_0^2}{\sigma_0^2 + \sigma^2/n} \right) \hat{\theta} + \left(\frac{\sigma^2/n}{\sigma_0^2 + \sigma^2/n} \right) \theta_0 \quad (5)$$

Thus, Bayesian estimates, $\hat{\theta}_B$, of the model parameters can be obtained throughout the sequence, with accuracy increasing with time after the mainshock. Immediately after the mainshock, the calculation of $\hat{\theta}_B$ heavily weights the a priori mean parameter value; during the course of the aftershock sequence, the a posteriori parameter estimates are increasingly weighted as the current data become more numerous and σ^2/n becomes small compared to σ_0^2 . Monte Carlo simula-

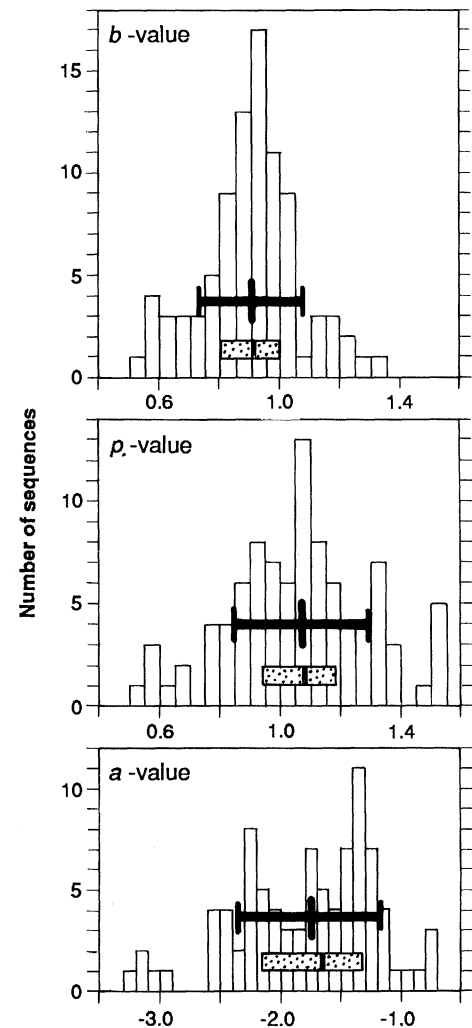


Fig. 2. Distributions of parameters (b , p , and a) determined for aftershock sequences following 62 ($M \geq 5.0$) mainshocks in California from 1933 to 1987. Solid bar indicates mean ± 1 sd. Shaded bar indicates median (central line) and upper and lower quartiles (end points) of distribution.

tions indicate that, for the generic California sequence, the a posteriori parameter estimates receive more than half the total weight within approximately 24 hours. Thus, immediately useful and increasingly accurate estimates of probabilities for aftershocks or larger mainshocks can be obtained during an ongoing earthquake sequence.

Our statistical model is completely general, and can be easily extended to other geographic or tectonic regions; only the a priori parameter values are particular to California. The ability to estimate param-

eters for an ongoing sequence, however, obviously depends on the availability of network processing with the capability to locate epicenters and to estimate magnitudes accurately in real time.

In the present model, the estimated values of the parameters are essentially determined from the smaller magnitude earthquakes. Justification for extending the model to larger magnitudes is provided by the close agreement between the estimated probability for larger mainshocks that we determined and the observed foreshock frequency in

southern California. Furthermore, the model should be applicable at larger magnitudes for a self-similar process, and California seismicity is apparently self-similar over a wide range of magnitudes (27). Although there is some evidence that the Gutenberg-Richter magnitude relation may systematically underestimate the number of larger magnitude earthquakes worldwide (7), it adequately accounts for the California data.

We have adopted a simple inverse power-law time decay to describe aftershock rate. More sophisticated models with more parameters—such as trigger and epidemic models, models allowing for secondary or multiple aftershock sequences, and those based on a combination of power-law and exponential time decays—may be appropriate for modeling some complete sequences that include numerous observations (28, 29). However, we preferred to develop a simple model to ensure that the estimation of parameters is stable during the early hours of an ongoing aftershock sequence when precious few data are available from which to infer a larger number of parameters.

The simplification of the spatial distribution of aftershocks described above precludes any inference of the detailed spatial distribution of aftershocks or larger mainshock (30). However, from the standpoint of early hazard evaluation, detailed spatial resolution of the expected earthquake activity may be effectively limited by a lack of knowledge about the mainshock faulting process. As such data become available in the days following the mainshock, appropriate corrections to the isotropic results could be applied.

Table 1. Interval probabilities, $P(M_1, M_2, S, T)$ for the generic California aftershock sequence for strong aftershocks or larger mainshocks ($M_1 = M_m - 1, M_2 = \infty$), and for larger mainshocks only ($M_1 = M_m, M_2 = \infty$). Time intervals are described by S (interval start time, in days after the mainshock) and $(T - S)$ (duration, in days). Model parameters for the generic sequence are ($b = 0.91, p = 1.08, a = -1.67, c = 0.05$).

$(T-S)$	S								
	0.01	0.25	0.50	1	3	7	15	30	60
<i>Earthquakes with $M \geq M_m - 1$</i>									
1	0.234	0.119	0.083	0.052	0.021	0.009	0.004	0.002	0.001
3	0.296	0.181	0.140	0.100	0.049	0.024	0.012	0.006	0.003
7	0.338	0.227	0.186	0.144	0.083	0.046	0.025	0.013	0.007
30	0.399	0.297	0.258	0.217	0.152	0.104	0.068	0.042	0.024
60	0.424	0.326	0.289	0.249	0.185	0.136	0.096	0.064	0.039
90	0.437	0.342	0.305	0.267	0.203	0.154	0.113	0.079	0.051
365	0.479	0.390	0.357	0.320	0.261	0.214	0.173	0.137	0.103
1000	0.504	0.420	0.388	0.353	0.297	0.252	0.212	0.177	0.142
<i>Earthquakes with $M \geq M_m$</i>									
1	0.032	0.015	0.011	0.007	0.003	0.001	0.001	0.000	0.000
3	0.042	0.024	0.018	0.013	0.006	0.003	0.001	0.001	0.000
7	0.049	0.031	0.025	0.019	0.011	0.006	0.003	0.002	0.001
30	0.061	0.042	0.036	0.030	0.020	0.013	0.009	0.005	0.003
60	0.066	0.047	0.041	0.035	0.025	0.018	0.012	0.008	0.005
90	0.068	0.050	0.044	0.037	0.028	0.020	0.015	0.010	0.006
365	0.077	0.059	0.053	0.046	0.036	0.029	0.023	0.018	0.013
1000	0.083	0.065	0.059	0.052	0.042	0.035	0.029	0.024	0.019

Table 2. Interval probabilities, $P(M_1, M_2, S, T)$, for strong aftershocks or a larger mainshock ($M_1 = M_m - 1, M_2 = \infty$), following the 1987 ($M = 5.9$) Whittier-Narrows, CA, earthquake and the 1983 ($M = 6.5$) Coalinga, CA, earthquake. Time intervals are described by S (interval start time, in days after the mainshock) and $(T - S)$ (duration, in days). Model parameters for the Whittier-Narrows earthquake data were $a = -1.60, b = 0.73, p = 1.50$, and $c = 0.05$ and for the Coalinga earthquake data were $a = -1.47, b = 0.89, p = 1.06$, and $c = 0.05$.

$(T-S)$	S								
	0.01	0.25	0.50	1	3	7	15	30	60
<i>Whittier-Narrows ($M = 5.9$) Sequence; Earthquakes with $M \geq 4.9$</i>									
1	0.393	0.141	0.084	0.044	0.012	0.004	0.001	0.000	0.000
3	0.431	0.185	0.123	0.074	0.026	0.010	0.004	0.001	0.000
7	0.448	0.208	0.146	0.095	0.040	0.017	0.007	0.003	0.001
30	0.465	0.232	0.171	0.120	0.062	0.034	0.017	0.009	0.004
60	0.470	0.238	0.178	0.127	0.069	0.040	0.023	0.012	0.006
90	0.472	0.241	0.181	0.130	0.073	0.043	0.025	0.015	0.008
365	0.476	0.248	0.188	0.138	0.080	0.051	0.033	0.021	0.013
1000	0.478	0.250	0.191	0.141	0.083	0.054	0.036	0.024	0.016
<i>Coalinga ($M = 6.5$) Sequence; Earthquakes with $M \geq 5.5$</i>									
1	0.330	0.176	0.125	0.081	0.033	0.015	0.007	0.003	0.002
3	0.413	0.265	0.209	0.153	0.077	0.039	0.020	0.010	0.005
7	0.467	0.330	0.276	0.218	0.129	0.074	0.040	0.022	0.011
30	0.545	0.427	0.378	0.324	0.234	0.165	0.109	0.069	0.039
60	0.577	0.466	0.420	0.370	0.283	0.214	0.154	0.105	0.066
90	0.593	0.487	0.443	0.394	0.310	0.242	0.181	0.130	0.086
365	0.643	0.550	0.511	0.468	0.393	0.332	0.274	0.221	0.169
1000	0.673	0.588	0.552	0.513	0.444	0.387	0.334	0.283	0.233

REFERENCES AND NOTES

1. Utsu (2) defines "aftershock" as follows: "It is often observed that a number of earthquakes occur in a group within a limited interval of time and space. The largest earthquake in such a series is called the mainshock, and smaller ones occurring before and after the mainshock are called foreshocks and aftershocks respectively." Such a retrospective definition requires observation of the entire sequence (so that the largest earthquake in the series can be determined). In this study, we assume that a large earthquake has recently occurred, and refer to it as the "mainshock." We refer to smaller earthquakes that may follow it as "aftershocks," and any larger earthquake that may follow as a "larger mainshock."
2. T. Utsu, *J. Fac. Sci. Hokkaido Univ. Ser. 7* **3**, No. 3 (1969).
3. L. M. Jones, *Bull. Seismol. Soc. Am.* **75**, 1669 (1985). Foreshocks in this study were limited to earthquakes within 10 km of the mainshock epicenter.
4. J. Goltz, *The Parkfield and San Diego Earthquake Predictions: A Chronology, Report of the Southern California Earthquake Preparedness Project* (Governor's Office of Emergency Services, Sacramento, CA, 1985).
5. T. Utsu, *Geophysics* **30**, 521 (1961).
6. ———, *J. Fac. Sci. Hokkaido Univ. Ser. 7* **3**, No. 4 (1970).
7. ———, *ibid.* **3**, No. 5 (1971).
8. ———, *ibid.* **4**, No. 1 (1972).
9. ———, *J. Phys. Earth* **22**, 71 (1974).

10. P. A. Reasenber, *J. Geophys. Res.* **90**, 5479 (1985).
11. Data were obtained from catalogs prepared separately for southern and eastern California (12), northern California before 1971 (13), and northern California after 1971 (14). A variety of magnitude scales have been used in California. For mainshocks ($M \geq 5.0$), M_W (moment magnitude) was used when available; otherwise M_L (local magnitude) was used. For southern and eastern California aftershocks, we used M_L for ($M \geq 3.0$), and M_{CA} (coda amplitude magnitude) for ($M < 3.0$). For northern California aftershocks, we used M_L before 1970 and M_D (coda duration amplitude) after 1970.
12. D. D. Given, L. K. Hutton, L. M. Jones, *U.S. Geol. Surv. Open-File Rep.* 87-488 (1987).
13. R. B. Darragh *et al.*, *Bull. Seismographic Stations Univ. Calif., Berkeley* **55**, 1-2 (1985).
14. S. L. Kirkman-Reynolds and F. W. Lester, *U.S. Geol. Surv. Open-File Rep.* 86-157 (1987).
15. This algorithm identifies clusters of earthquakes in time and space. By defining the identified clusters as the set of aftershocks, we effectively eliminate the spatial part of the problem. Thus, from this point on, the analysis considers aftershocks as two-dimensional (time-magnitude) vectors.
16. We used $c = 0.05$ days, the value that minimizes χ^2 for the post-1970 data.
17. Errors are ± 1 standard deviation of the mean.
18. Subsets of sequences occurring in each tectonic regime in California were compared with the two-sample t test for difference in the mean of each parameter; $\bar{a}_{east} > \bar{a}_{north}$, $p < 0.02$ and $\bar{a}_{east} > \bar{a}_{south}$, $p < 0.005$.
19. Sensitivity of the calculated probabilities to variations in the model parameters was investigated. A 10% increase in a , b , c , or p , relative to the generic value, leads to probabilities for strong aftershocks at $S = 1$, $(T - S) = 365$ of 0.44, 0.35, 0.32, and 0.25, respectively, compared to the generic probability of 0.32 in Table 1. Corresponding probabilities for larger mainshocks are 0.068, 0.042, 0.046 and 0.035, compared to the generic probability 0.046 in Table 1.
20. L. M. Jones and P. A. Reasenber, *Eos* **69**, 1305 (1988).
21. J. Bennett and R. Sherburne, Eds., *Calif. Div. Mines Geol. Spec. Pub.* 66 (1983).
22. E. Hauksson *et al.*, *Science* **239**, 1409 (1988).
23. W. Ellsworth and M. Rymer, Eds., *U.S. Geol. Surv. Prof. Pap.* 1487 (1988).
24. We obtained the probability estimates given in Table 2 using parameters estimated for the entire earthquake sequences; thus, they are generally better-determined than those that would have been obtained in real-time during the earthquake sequences. We present these best model estimates of aftershock probability rather than the real-time or "limited knowledge" estimates in order to best demonstrate the time- and magnitude-dependence of the calculated probabilities and to provide a uniform comparison of results for these contrasting earthquake sequences.
25. R. T. Hogg and A. T. Craig, *Introduction to Mathematical Statistics* (Macmillan, New York, 1978).
26. A. H. Bowker and G. J. Lieberman, *Engineering Statistics* (Prentice Hall, Englewood Cliffs, New Jersey, ed. 2, 1972).
27. Y. Y. Kagan and L. Knopoff, *J. Geophys. Res.* **86**, 2853 (1981).
28. Y. Ogata, *J. Phys. Earth* **31**, 115 (1983).
29. ———, *J. Am. Stat. Assoc.* **83**, 9 (1988).
30. The empirical (isotropic) spatial distribution of strong aftershocks in California was determined from the California data. The median distance between $M \geq 5.0$ aftershocks and their mainshock epicenter is 5 km. The 80 percentile distance is 9 km.
31. We thank M. V. Matthews for providing technical assistance throughout the study, B. Ellsworth and Y. Ogata for helpful discussions and suggestions, and R. D. Brown, for initially stimulating our interest in this problem.

20 September 1988; accepted 23 December 1988

Time and Spatial Dependence of the Concentration of Less Than 10^5 Microelectrode-Generated Molecules

STUART LICHT, VINCE CAMMARATA, MARK S. WRIGHTON*

The time and spatial dependence of the concentration of as few as 40,000 electrogenerated, redox-active molecules has been determined. The distance between generator and detector microelectrodes in an array used in the study could be varied from 0.8 to 28 micrometers. Measurements of a sufficiently small ensemble of molecules allowed the experimental results to be compared with a quantitative simulation of the random movement of each member of the ensemble. The transit time of an electrogenerated species from the generator to a collector microelectrode was measured as a function of viscosity, diffusivity, and distance.

MICROELECTROCHEMICAL DEVICES can be used in the study of catalysis, energy conversion, sensors, displays, and molecule-based electronics (1-4). In 1984 Kittlesen and Wrighton introduced the microfabrication of arrays of closely spaced, individually addressable micrometer-dimensioned electrodes (5) and their subsequent modification to fabricate molecule-based transistors, diodes, and sensors (6). In biological systems in which electrochemical stimulation or monitoring is useful, such as in the release of drugs and neurotransmitters (7), the use of microelectrodes may prove useful for creating and monitoring chemical signals. Another goal of such research is to reduce the size of the ensemble of electrogenerated species so that discrete electrochemical events can be measured.

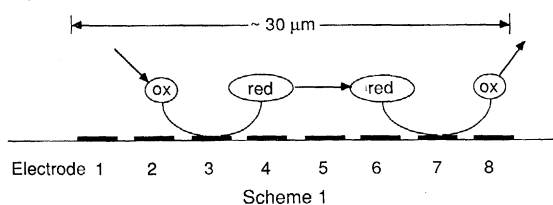
We have used an array of closely spaced ($\sim 1 \mu\text{m}$), individually addressable micro-

electrodes ($< 10^{-7} \text{ cm}^2$ in area) to monitor the time and spatial dependence of $< 10^5$ electrogenerated species. We have directly measured the dynamics associated with diffusing species on a sufficiently small scale ($< 30 \mu\text{m}$) and of sufficiently few species ($< 10^5$) that the measurements can be compared with a quantitative simulation of the random movement of each species. Studies of the dynamics of electrogenerated species in the solid state and other media not accessible by traditional electrochemical methods, such as rotating ring-disk electrodes, should now be possible (8).

Electrochemical methods have been used to monitor the diffusion of electrogenerated species. The concentration profile within the diffusion layer near a macroelectrode can be mapped to within $\sim 5 \mu\text{m}$ with a movable light source (9) or a movable microelectrode (10). Microelectrodes have been used to monitor the time of flight of a pulse of 10^{-6} C through a variety of thin films overcoating the microelectrodes (11). Our smaller microelectrodes allow these diffusion studies to be extended to a qualitatively smaller amount of electrogenerated material.

Recently, Bard *et al.* demonstrated that in steady-state experiments a large fraction of redox-active material generated at one microelectrode can be detected or "collected" at nearby microelectrodes (12). We show here that the transit time for movement of the electrogenerated species from generator to collector is a measure of the diffusion characteristics of the electrogenerated solution species. A redox-active species is generated at one electrode, diffuses, and is collected at a second electrode (Scheme 1). Procedures used in the microfabrication and pretreatment of the gold microelectrode arrays are similar to those described in (13, 14).

The experimental in situ spatial and tem-



Scheme 1. Representation of generation-collection experiments at a microelectrode array where "generation" can be effected at any one of the microelectrodes and "collection" can be done at any other microelectrode. The potential at electrode 3 is pulsed to "generate" an ensemble of reduced species. The potential at electrode 7 is fixed to "collect" a fraction of the reduced species by oxidation.

Department of Chemistry, Massachusetts Institute of Technology, Cambridge, MA 02139.

*To whom correspondence should be addressed.